Archives of Gynecology and Obstetrics (2019) 299:1459–1465
https://doi.org/10.1007/s00404-019-05108-w

GYNECOLOGIC ONCOLOGY

Neurovascular and lymphatic vessels distribution in uterine ligaments based on a 3D reconstruction of histological study: to determine the optimal plane for nerve-sparing radical hysterectomy

Pengfei Li[1] · Hui Duan[1] · Jun Wang[1] · Shipeng Gong[1] · Guidong Su[1] · Jianyi Li[2] · Lei Tang[2] · Yan Zhang[3] · Huijian Fan[1] · Ping Liu[1] · Chunlin Chen[1]

Received: 24 July 2018 / Accepted: 4 March 2019 / Published online: 14 March 2019

Abstract

Objective To present the distribution of neurovascular and lymphatic vessels in uterine ligaments using 3D models based on the pathological staining of serial 2D sections of postoperative specimens.

Methods Serial transverse sections of fresh uterine ligaments from a patient with stage IB1 cervical squamous cell carcinoma were studied using the computer-assisted anatomic dissection (CAAD) technique. The sections were stained with hematoxylin and eosin, Weigert elastic fibers, D2-40 and immunostainings (sheep anti-tyrosine hydroxylase and rabbit anti-vasoactive intestinal peptide). The sections were then digitalized, registered and reconstructed three-dimensionally. Then, the 3D models were analyzed and measured.

Results The 3D models of the neurovascular and lymphatic vessels in uterine ligaments were created, depicting their precise location and distribution. The vessels were primarily located in the upper part of the ligaments model, while the pelvic autonomic nerves were primarily in the lower part; the lymphatic vessels were scattered in the uterine ligaments, without obvious regularity.

Conclusion CAAD is an effective anatomical method to study the precise distribution of neurovascular and lymphatic vessels in uterine ligaments. It can present detailed anatomical information about female pelvic autonomic innervation and the spatial relationship between nerves and vessels and may provide a better understanding of nerve-sparing radical hysterectomy.

Keywords Cervical cancer · Nerve-sparing · Pelvic autonomic nerves · 3D reconstruction · Histological examination

Introduction

Cervical cancer ranks as the fourth most common cancer in women worldwide and remains one of the main causes of cancer death in developing countries [1]. Radical hysterectomy (RH) is an effective treatment for early stage cervical cancer (Ia2–IIa2), and postoperative patients have high survival rates and low recurrence rates, but up to 30–80% of these patients may suffer from significant bladder, rectal or sexual dysfunction [2, 3]. Intraoperative injury of pelvic autonomic nerves (PAN) is widely regarded as one of the main causes of these complications [4].

Since Okabayashi proposed the idea of preserving nerve in radical hysterectomy in 1921, the technique for nerve-sparing is gradually gaining the attention of gynaecological oncologists, which may reduce these complications mentioned above. Kobayashi preserved pelvic splanchnic nerves during the resection of cardinal ligaments in 1961, and the surgical

Pengfei Li, Hui Duan and Jun Wang contributed equally to this work.

✉ Ping Liu
lpivy@126.com

✉ Chunlin Chen
ccl1@smu.edu.cn

[1] Department of Obstetrics and Gynecology, Nanfang Hospital, Southern Medical University, No. 1838, Guangzhou Avenue, Guangzhou 510515, China

[2] Department of Anatomy, Guangdong Province Key Laboratory of Medical Biomechanics, School of Basic Medicine Science, Southern Medical University, Guangzhou, China

[3] Department of Pathology, Nanfang Hospital, Southern Medical University, Guangzhou, China

procedure was published in English by Sakamoto et al. in 1988 [5]. With respect to the course of the pelvic plexus, Höckel developed a surgical technique for radical hysterectomy intended to compromise between maximum parametrial radicalness and sustained pelvic autonomic nerve function [6, 7]. Although the safety and effectiveness of nerve-sparing radical hysterectomy (NSRH) have been confirmed [8–10], detailed surgical procedures and defined surgical anatomy have also been provided, NSRH have not been widely used in clinical practice. Because the procedures of intraoperative nerve identification are difficulties during NSRH [11], many surgeons begin to perform this surgery through the mode of "learning by doing", confused by whether the nerves preserved are actually true nerves.

For better nerve identification, several studies have focused on the type of nerve fibers and the distribution of nerves in ligaments by histological examination. To a certain extent, readers can speculate on the three-dimensional (3D) distribution of the PAN from two-dimensional (2D) histologic neuroquantitative examinations, according to these studies [12–14]. But different studies drew different conclusions and sometimes completely opposite conclusions [13, 14]. The reason for this phenomenon is that the methods used for taking ligament specimens differed among the various studies. We proposed that some cardinal ligaments were taken when obtaining uterosacral ligament specimens, and some cardinal ligament specimens were only taken from a part of the ligament. In some studies, the 3D pelvic autonomic nerve model was constructed based on pathological staining of fetal specimens [15, 16], presenting intuitively the 3D distribution of PAN, but the pelvic structure of the fetus is different from that of the adult. Thus, current studies do not offer practical assistance for understanding PAN innervation in uterine ligaments,or they do not provide guidance on surgery implementation, but they do help direct future research.

Thus, the aim of this study is to establish 3D reconstruction of neurovascular and lymphatic vessels in uterine ligaments based on the pathological staining f serial 2D sections using the computer-assisted anatomic dissection (CAAD) technique. Reconstruction of these 3D models of uterine ligaments may contribute to a better understanding of the complex neurovascular distribution and their mutual spatial relationship, which could serve as an essential anatomical basis to standardize the performance of NSRH and may help to determine an optimal plane for NSRH.

Materials and methods

Specimen collection

Fresh uterine ligament specimens were obtained from a patient with stage IB1 cervical squamous carcinoma, who underwent abdominal radical hysterectomy (Piver type III) in August 2014. Parametrial invasion was not detected by preoperative MRI examination. The patient had no history of radiotherapy or chemotherapy before the operation. Ethical approval for the study was obtained from the ethics committee of Nanfang Hospital, Southern Medical University, and the patient was informed and agreed in writing to this study.

The cardinal ligament, uterosacral ligament, and paracolpium accompanied by and part of the cervical tissue on the contralateral side of the tumor, were taken as a whole, and the length, width and thickness of the ligaments were measured. To distinguish between diffident ligaments in the 3D reconstruction process, the facies lateralis of the uterosacral ligaments and the upper side of the specimens were marked with India ink. The pelvic side of the ligaments was sent to the pathology department to detect whether the ligaments had tumor invasion.

Macroscopic dissection

The samples and a position rod were fixed in a 10% formaldehyde solution and embedded with paraffin. Four rectangular normal pig liver tissues, with a diameter of 0.3 cm, were set parallel to the position rod in the process of paraffin fixation. Serial transversal cross-sections were made from the specimen in 5 μm sections, and five sections, each being 100 μm of specimen, were taken, and a total of 1287 sections were gained. Each five serial sections in 1287 sections were divided into one group. In addition, according to the requirements of the pathologist, sections from different parts of the ligament were sent to exclude tumor invasion.

Histological examination

In each group, the first section was stained with hematoxylin–eosin (HE) staining to distinguish vessels, the second section was stained with Weigert (elastic fibers) staining to distinguish the arteries from vessels, the third and the fourth sections were selected for immunohistochemical analysis by sheep anti-tyrosine hydroxylase (TH) and rabbit anti-vasoactive intestinal peptide (VIP) to identify sympathetic adrenergic fibers and sympathetic adrenergic fibers, respectively, and the fifth section was stained with D2-40 to mark lymphatic vessels. The TH (Code No.LV1458671, Chemicon, USA) was diluted to 1/800, and the VIP (Code No. SC-25347, Santa Cruz, USA) was diluted to 1/50. The histological examination protocol was the same as previously reported [12].

Image collection

All of the different stainings of serial section images were scanned with the Motic BA600 MOT-7.5 automated

microscope (Motic, Fujian, China). The sections were first scanned 2 × 10 times under the map; automatic scanning was achieved when the ocular lens was adjusted to 10 × 10 times. Pictures were saved in BMP format.

Image registration and analysis

Adobe Photoshop image processing software CS5.1 (Adobe Systems, California, USA) was used to separate the images of the position rods, and then Matlab software (Math Works, Massachusetts, USA) was used to realize image automatic registrations; Adobe Photoshop image processing software was also used for fine adjustment. When all images were registered, five sets of serial images were imported in Adobe Photoshop software to manually draw the contours of arteries, veins, sympathetic nerves, parasympathetic nerves and lymphatic vessels. Then, all the pictures were adjusted to the appropriate size using ACDSEE software (ACD Systems, British Columbia, Canada).

3D reconstruction

Five sets of images were imported into Mimics 10.01 software (Materialise, Leuven, Belgium) to complete 3D reconstruction. Two-dimensional (2D) image segmentation was necessary for 3D reconstruction. The 2D segmentation of ligaments, arteries, veins, sympathetic nerves, parasympathetic nerves and lymphatic vessels was accomplished using the 'draw tool' of Mimics based on tissue contours drawn previously by Adobe Photoshop image processing software. When segmentation was complete, the 3D representations of the 2D segmentation were created using Mimics' '3D calculation' function. For better visualization, transparent operation of the 3D ligaments model was performed with Mimics' 'transparent tool'.

Once all of the procedures were finished, 3D reconstruction of neurovascular and lymphatic vessels in uterine ligaments was obtained. Then, based on the size of the specimen measured before, the 3D models of ligaments were adjusted to the same size. The indexes of interest were measured with Mimics' measurement tools (Fig. 1a–f).

Results

The 3D models of neurovascular and lymphatic vessels in uterine ligaments based on pathological staining of serial 2D sections were created using the CAAD technique. From the 3D models, it was found that the uterine ligaments and paracolpium contained abundant vessels, autonomic nerves and lymphatic vessels. The 3D model of the cardinal ligament and paracolpium was 42.0 mm in length, 35.0 mm in width and 4.2 mm in thickness (Fig. 2a–c). The 3D model

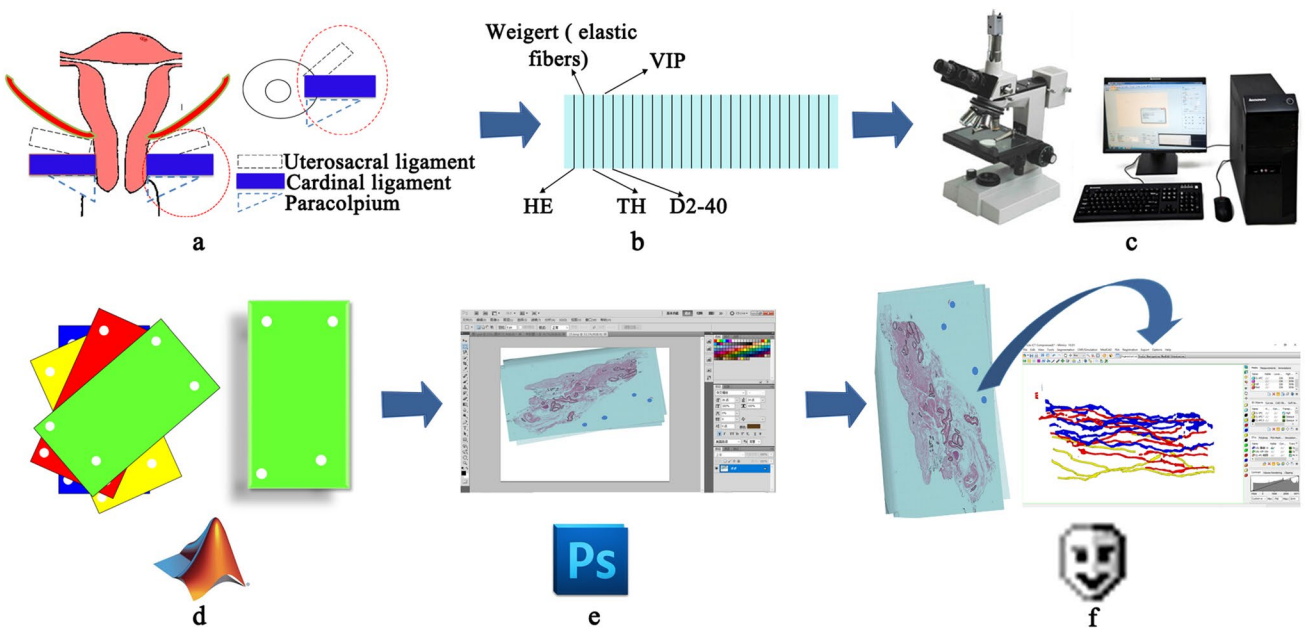

Fig. 1 The procedure of creating 3D models of neurovascular and lymphatic vessels in uterine ligaments is shown. The cardinal ligament, uterosacral ligament, and paracolpium accompanied by and part of the cervical tissue were taken as a whole (**a**). Serial transversal cross-sections were taken and different staining of serial section images were collected (**b**, **c**). Matlab software was used to realize image automatic registrations, Adobe Photoshop image processing software was used for image analysis, and Mimics software was used to complete 3D reconstruction

of the uterosacral ligament was 37.1 mm in length, 25.2 mm in width and 4.0 mm in thickness.

The vessels were found to be primarily located in the upper part of ligament model, in either the cardinal ligament and paracolpium or uterosacral ligament. The diameter of vessels in the cardinal ligament and paracolpium was larger than that in the uterosacral ligament. In the proximal, middle and distal segments of the ligament, the distances from the vessels to the upper edge of the ligament were measured as shown in Fig. 2e–i.

The PAN was primarily found in the lower part of the ligament model, in either the cardinal ligament and paracolpium or the uterosacral ligament. The cardinal ligament and paracolpium contained both sympathetic nerves and parasympathetic nerves, but there were more sympathetic nerves than parasympathetic nerves. There were only sympathetic nerves found in the lateral portion of the sacral ligament. In the proximal, middle and distal segments of ligament, the distances from the nerves to the upper edge of the ligaments were measured as shown in Fig. 2j–m. In the proximal, middle and distal segments of the cardinal ligament and paracolpium, the distances between the nerves and the vessels were 0.50 mm, 1.90 mm, and 3.10 mm, respectively (Fig. 2n).

The distribution of the lymphatic vessels in the uterine ligaments was scattered, without obvious regularity. There

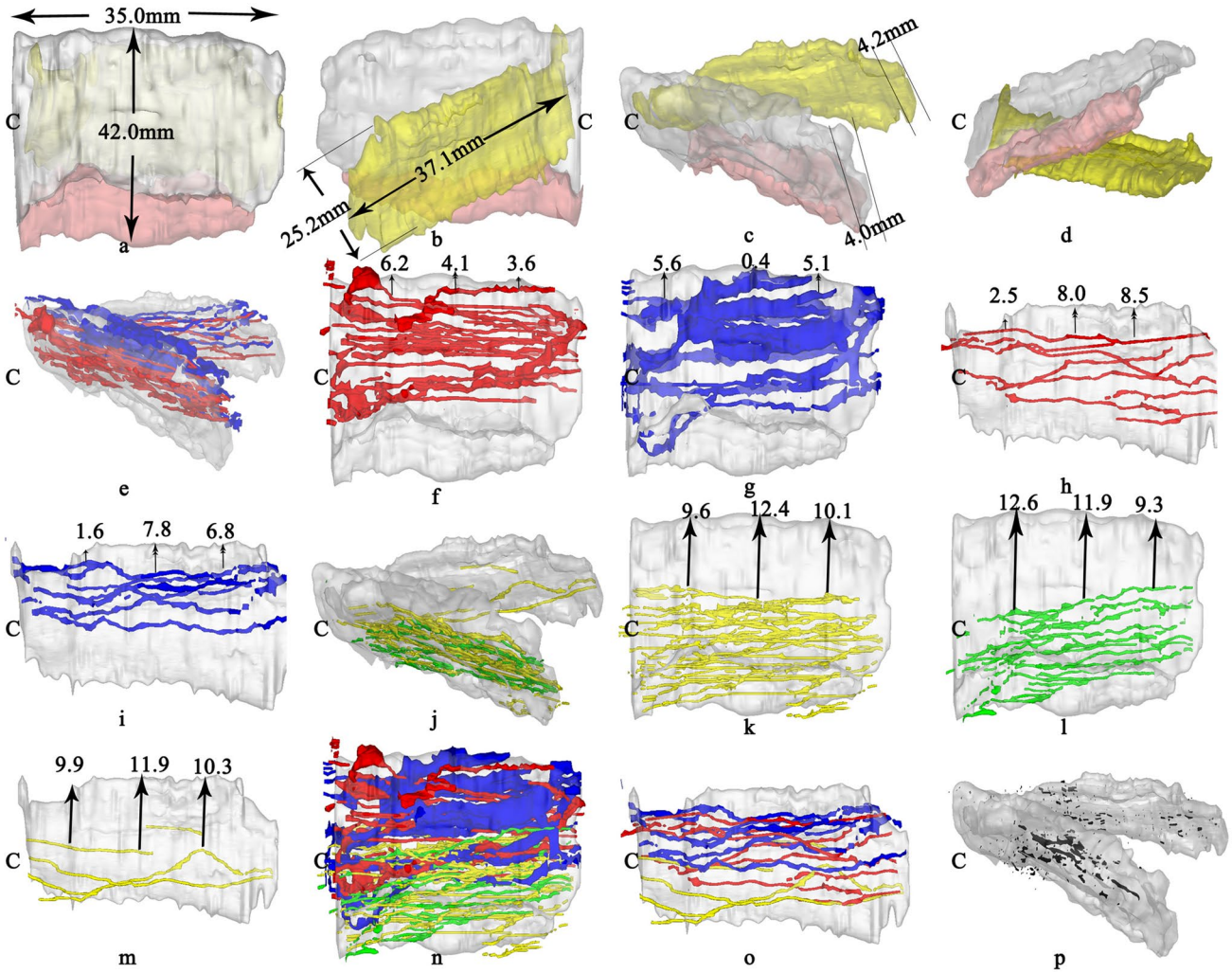

Fig. 2 3D models of neurovascular and lymphatic vessels in uterine ligaments are shown. The 'C' indicates the cervical lateral of ligaments. 3D model of uterine ligaments and their measurement was presented (white represents cardinal ligament, yellow represents uterosacral ligament, and pink represents paracolpium), the cardinal ligament was connected to paracolpium (**a**–**d**). **e** The distribution of vessels in uterine ligaments, **f** and **g** the distribution of arteries and veins in cardinal ligament and paracolpium, respectively, **h**, **i** the distribution of arteries and veins in uterosacral ligament, respectively. **j** The distribution of nerves in uterine ligaments, **k**, **l** the distribution of sympathetic nerves and parasympathetic nerves in cardinal ligament and paracolpium, respectively, **m** The distribution of sympathetic nerves in uterosacral ligament. **n** The distribution of neurovascular in cardinal ligament and paracolpium, **o** the distribution of neurovascular in uterosacral ligament. **p** The distribution of lymphatic vessels in uterine ligaments

were more lymphatic vessels located in the uterosacral ligament than in the cardinal ligament and paracolpium.

Discussion

In this study, we successfully constructed 3D models of neurovascular and lymphatic vessels in uterine ligaments, measured the distances from the vascular and nerve trunks to the upper edge of the ligaments, and analyzed the distances between vessels and nerves. According to the previous studies [5, 6, 10], the key steps of NSRH is to preserve the hypogastric nerves, located in the lateral portion of the sacrouterine ligament, the pelvic splanchnic nerves, located on the dorsal side of the cardinal ligament, and the inferior hypogastric plexus and its branches supplied to bladder and rectum, fused by hypogastric nerves and pelvic splanchnic nerves, so as to reduce functional defects in bladder and/or bowel. From the 3D models, we could also instinctively observe that the vessels ran in the upper part of the cardinal ligament, the nerves ran in the lower part of the cardinal ligament, and the nerves ran in the lateral portion of the sacrouterine ligament. If NSRH was carried out on this patient, retaining the nerves does not preserve all of the nerves, but retaining nerve trunks on the nerves' surface is in the cardinal ligament (Fig. 3a) and the lateral portion of the uterosacral ligament (Fig. 3b). This study explained the feasibility of NSRH because there was a certain distance between nerve trunks and vascular trunks in uterine ligaments. This study also verified the theory of Kobayashi [17], who divided the cardinal ligament into the vascular part and the neural part according to clinical experience. The lymphatic vessels were scattered in the uterine ligaments, without obvious regularity in the 3D models, but we can use other techniques to achieve intraoperative visualization and navigation of lymphatic vessels in the uterine ligaments, intraoperative injection of indocyanine-green into cervix or corpus is one of the effective techniques [18]. For surgeons, the 3D models may provide a better understanding of the neurovascular anatomy and the surgical procedures of NSRH [19].

Several previous studies have also quantitatively analyzed the distribution of vessels and nerves in the uterine ligaments by 2D pathological examination, but different studies have drawn different conclusions [12–14]. For example, Butler-Manuel et al. [13] deemed that there were two types of sympathetic nerves and parasympathetic nerves in cardinal ligaments, while Tomoyasu Kate et al. [14] stated that the nerve part of the cardinal ligament was made up of collagen connective tissue that did not contain parasympathetic nerves (pelvic splanchnic nerves), and pelvic splanchnic nerves were carried on the dorsal side of the cardinal ligaments. We analyzed this and determined that this discrepancy was due to the use of different specimen collection methods. In some studies of uterosacral ligaments, parts of cardinal ligaments were taken, resulting in different types of nerve fibers in the ligaments. In some studies of cardinal ligaments, specimens only consisted of a part of the ligament, so the pelvic visceral nerves were not included. The 3D visualization of the cervical ligament as a whole can solve the above problems.

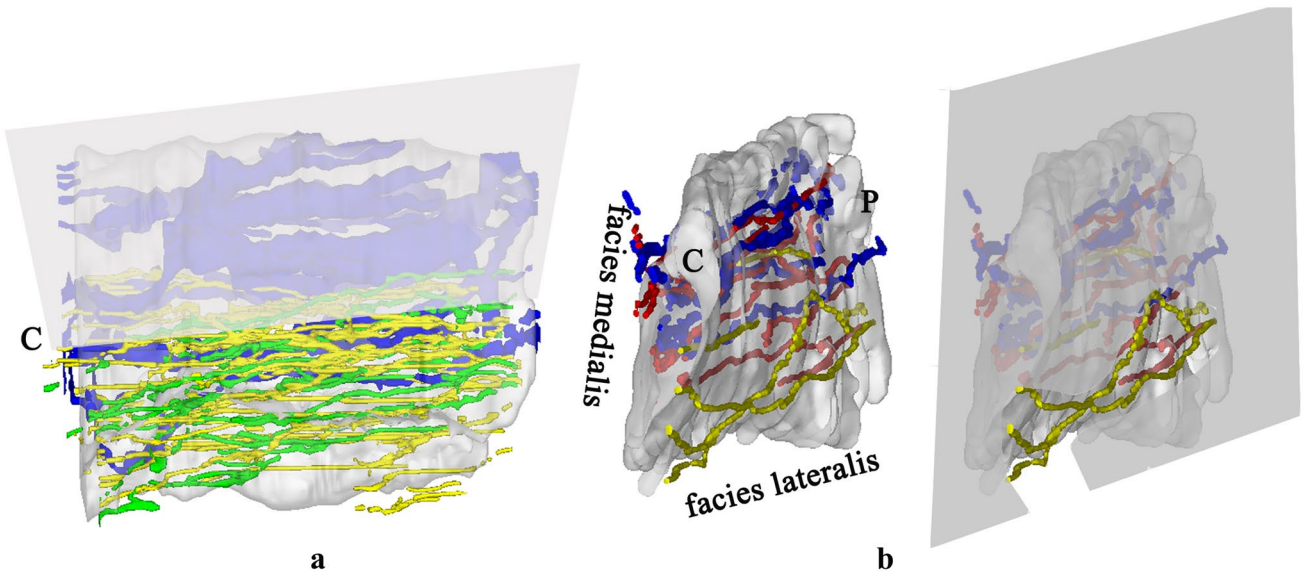

Fig. 3 If NSRH was carried out on this patient, the optimal plane for NSRH is shown: retaining nerve trunks on the nerves' surface is in the cardinal ligament (**a**) and the lateral portion of the uterosacral ligament (**b**). The 'C' indicates the cervical lateral of ligaments, the 'P' indicates the pelvic lateral of ligaments. The gray rectangle indicates the optimal plane for NSRH

Studies focused on the 3D reconstruction of pelvic autonomic nerves based on aborted fetal specimens performed 3D visualization of the PAN, but the proportions of the pelvic organs of the fetus are different from that of the adult, and thus, these studies were shown to be of no obvious help in understanding the NSRH operation [15–17, 20]. Different from fetal bone registration in the study of fetal specimens, we used pig liver tissues as a position rod in the process of 3D reconstruction. Since in our previous studies, we have compared the removal rate of pig liver, hair and suture silk during pathological examination, it is found that the liver tissue is a better rod material.

The 3D reconstructions of in vivo PAN and their related organs based on MRI may provide 3D anatomical information on the PAN and guidance on the identification of nerves during NSRH, but it was only a proof of concept report of the new application of MRI on in vivo PAN and failed to assess whether the nerves constructed were actually true nerves [21]. In this study, we constructed 3D models of neurovascular and lymphatic vessels in uterine ligaments by histological examination and the CAAD technique, presenting accurate female pelvic autonomic innervation and the spatial relationship between nerves and vessels in uterine ligaments.

In the process of specimen collection and macroscopic dissection, the pelvic side of the ligaments and sections from different parts of the ligaments were sent to the pathology department to confirm that the ligaments had not been invaded by tumor. The postoperative treatment plan of the patient was not affected by this study. In addition, it was reported that the specificity of preoperative MRI examination for evaluation of non parametrial invasion was more than 90% [22, 23]. The patient's preoperative MRI showed no parametrial invasion, suggesting that the possibility of parametrial invasion is very small.

Some reports have suggested that the distribution of the PAN may vary between individuals, and the major limitation of this study was that there was only one specimen, so the 3D models were not representative of the neurovascular distribution in all individuals. And it cannot be shown that the nerves found in the specimen are nerves of rectum, bladder, uterus or vagina, since we established the 3D models of nerves in uterine ligaments, not all the inferior hypogastric plexus and its branches supplied to rectum, bladder, uterus and vagina, this may limit the value of 3D models. Plus, the creation of 1287 whole mount sections is technically difficult and time-consuming, making it is difficult to carry out a large-sample study.

Conclusion

In this study, we constructed 3D models of neurovascular and lymphatic vessels in uterine ligaments based on histological examination and the CAAD technique. The 3D models presented detailed anatomical information about female pelvic autonomic innervation and the spatial relationship between nerves and vessels in uterine ligaments, which may provide aids in understanding the complex surgical procedure of NSRH and guiding optimal plane for NSRH.

Acknowledgements This study has received funding by the National Natural Science Fund of China (81571422, 81370736), the National Science and Technology Support Program of China (2014BAI05B03), the National Natural Science Fund of Guangdong (2015A030311024), the Science and Technology Plan of Guangzhou (158100075), and the Foundation from the President of Nanfang Hospital of Southern Medical University (2015C015).

Author contributions PFL: protocol development, data collection and manuscript writing; HD: protocol development, data analysis and manuscript writing; JW: protocol development, data collection and manuscript writing; SPG: data analysis; GDS: data analysis; JYL: protocol development; LT: protocol development; YZ: protocol development; HJF: manuscript writing; PL: protocol development, data analysis and manuscript editing; CLC: protocol development, data analysis and manuscript editing.

Compliance with ethical standards

Conflict of interest The authors declare that they have no conflict of interest.

Ethical approval All procedures performed in studies involving human participants were in accordance with the ethical standards of the institutional and/or national research committee and with the 1964 Helsinki declaration and its later amendments or comparable ethical standards.

Informed consent Informed consent was obtained from the participant included in the study.

References

1. Koh WJ, Abu-Rustum NR, Bean S, Bradley K, Campos SM, Cho KR, Chon HS, Chu C, Clark R, Cohn D, Crispens MA, Damast S, Dorigo O, Eifel PJ, Fisher CM, Frederick P, Gaffney DK, Han E, Huh WK, Lurain JR 3rd, Mariani A, Mutch D, Nagel C, Nekhlyudov L, Fader AN, Remmenga SW, Reynolds RK, Tillmanns T, Ueda S, Wyse E, Yashar CM, McMillian NR, Scavone JL (2019) Cervical cancer, version 3.2019, NCCN clinical practice guidelines in oncology. J Natl Compr Canc Netw 17:64–84. https://doi.org/10.6004/jnccn.2019.0001
2. van Gent MD, Romijn LM, van Santen KE, Trimbos JB, de Kroon CD (2016) Nerve-sparing radical hysterectomy versus conventional radical hysterectomy in early-stage cervical cancer. a systematic review and meta-analysis of survival and quality of life. Maturitas 94:30–38. https://doi.org/10.1016/j.maturitas.2016.08.005
3. Wang X, Chen C, Liu P, Li W, Wang L, Liu Y (2018) The morbidity of sexual dysfunction of 125 Chinese women

following different types of radical hysterectomy for gynaecological malignancies. Arch Gynecol Obstet 297:459–466. https://doi.org/10.1007/s00404-017-4625-0
4. Balaya V, Rossi L, Cornou C, Ngô C, Bensaid C, Bats AS, Lecuru F (2017) Where does pelvic nerve injury occur during radical hysterectomy for cervical cancer? Gynecol Oncol 145:199–200
5. Sakamoto S, Takizawa K (1988) An improved radical hysterectomy with fewer urological complications and with no loss of therapeutic results for invasive cervical cancer. Baillieres Clin Obstet Gynaecol 2:953–962
6. Höckel M, Konerding MA, Peter Heuβel C (1998) Liposuction-assisted nerve-sparing extended radical hysterectomy: oncologic rationale, surgical anatomy, and feasibility study. Am J Obstet Gynecol 178:971–976. https://doi.org/10.1016/S0002-9378(98)70533-2
7. Höckel M, Horn LC, Hentschel B, Höckel S, Naumann G (2003) Total mesometrial resection: high resolution nerve-sparing radical hysterectomy based on developmentally defined surgical anatomy. Int J Gynecol Cancer 13:791–803. https://doi.org/10.1111/j.1525-1438.2003.13608.x
8. Aoun F, van Velthoven R (2015) Lower urinary tract dysfunction after nerve-sparing radical hysterectomy. Int Urogynecol J 26:947–957. https://doi.org/10.1007/s00192-014-2574-8
9. Kavallaris A, Hornemann A, Chalvatzas N, Luedders D, Diedrich K, Bohlmann MK (2010) Laparoscopic nerve-sparing radical hysterectomy: description of the technique and patients' outcome. Gynecol Oncol 119:198–201. https://doi.org/10.1016/j.ygyno.2010.07.020
10. van Gent MD, van den Haak LW, Gaarenstroom KN, Peters AA, van Poelgeest MI, Trimbos JB, de Kroon CD (2014) Nerve-sparing radical abdominal trachelectomy versus nerve-sparing radical hysterectomy in early-stage (FIGO IA2-IB) cervical cancer: a comparative study on feasibility and outcome. Int J Gynecol Cancer 24:735–743. https://doi.org/10.1097/IGC.0000000000000114
11. Kim HS, Kim TH, Suh DH, Kim SY, Kim MA, Jeong CW, Hong KS, Song YS (2015) Success factors of laparoscopic nerve-sparing radical hysterectomy for preserving bladder function in patients with cervical cancer: a protocol-based prospective cohort study. Ann Surg Oncol 22:1987–1995. https://doi.org/10.1245/s10434-014-4197-1
12. Chen C, Huang L, Liu P, Su G, Li W, Lu L, Wang L, Li X, Duan H, Zou C, Hatch K (2014) Neurovascular quantitative study of the uterosacral ligament related to nerve-sparing radical hysterectomy. Eur J Obstet Gynecol Reprod Biol 172:74–79. https://doi.org/10.1016/j.ejogrb.2013.09.035
13. Butler-Manuel SA, Buttery LD, A'Hern RP, Polak JM, Barton DP (2000) Pelvic nerve plexus trauma at radical hysterectomy and simple hysterectomy: the nerve content of the uterine supporting ligaments. Cancer 89:834–841. https://doi.org/10.1002/1097-0142(20000815)89:4%3c834:AID-CNCR14%3e3.0.CO;2-7
14. Kato T, Murakami G, Yabuki Y (2003) A new perspective on nerve-sparing radical hysterectomy: nerve topography and over-preservation of the cardinal ligament. Jpn J Clin Oncol 33:589–591
15. Kraima AC, Derks M, Smit NN, van de Velde CJ, Kenter GG, DeRuiter MC (2016) Careful dissection of the distal ureter is highly important in nerve-sparing radical pelvic surgery: a 3D reconstruction and immunohistochemical characterization of the vesical plexus. Int J Gynecol Cancer 26:959–966. https://doi.org/10.1097/IGC.0000000000000709
16. Moszkowicz D, Alsaid B, Bessede T, Penna C, Benoit G, Peschaud F (2011) Female pelvic autonomic neuroanatomy based on conventional macroscopic and computer-assisted anatomic dissections. Surg Radiol Anat 33:397–404. https://doi.org/10.1007/s00276-010-0773-7
17. Bertrand MM, Alsaid B, Droupy S, Benoit G, Prudhomme M (2013) Optimal plane for nerve sparing total mesorectal excision, immunohistological study and 3D reconstruction: an embryological study. Colorectal Dis 15:1521–1528. https://doi.org/10.1111/codi.12459
18. Kimmig R, Aktas B, Buderath P, Rusch P, Heubner M (2016) Intraoperative navigation in robotically assisted compartmental surgery of uterine cancer by visualisation of embryologically derived lymphatic networks with indocyanine-green (ICG). J Surg Oncol 113: 554–559. https://doi.org/10.1002/jso.24174
19. Bertrand MM, Macri F, Mazars R, Droupy S, Beregi JP, Prudhomme M (2014) MRI-based 3D pelvic autonomous innervation: a first step towards image-guided pelvic surgery. Eur Radiol 24:1989–1997. https://doi.org/10.1007/s00330-014-3211-0
20. Moszkowicz D, Alsaid B, Bessede T, Zaitouna M, Penna C, Benoit G, Peschaud F (2011) Neural supply to the clitoris: immunohistochemical study with three-dimensional reconstruction of cavernous nerve, spongious nerve, and dorsal clitoris nerve in human fetus. J Sex Med 8:1112–1122. https://doi.org/10.1111/j.1743-6109.2010.02182.x
21. Li P, Liu P, Chen C, Duan H, Qiao W, Ognami OH (2018) The 3D reconstructions of female pelvic autonomic nerves and their related organs based on MRI: a first step towards neuronavigation during nerve-sparing radical hysterectomy. Eur Radiol. https://doi.org/10.1007/s00330-018-5453-8
22. Thomeer MG, Gerestein C, Spronk S, van Doorn HC, van der Ham E, Hunink MG (2013) Clinical examination versus magnetic resonance imaging in the pretreatment staging of cervical carcinoma: systematic review and meta-analysis. Eur Radiol 23:2005–2018. https://doi.org/10.1007/10.1007/s00330-013-2783-4
23. Park JJ, Kim CK, Park SY, Park BK (2015) Parametrial invasion in cervical cancer: fused T2-weighted imaging and high-b-value diffusion-weighted imaging with background body signal suppression at 3 T. Radiology 274:734–741. https://doi.org/10.1148/radiol.14140920